

Evolution of the X-Ray Jets from 4U 1755–33

P. Kaaret¹, S. Corbel², J.A. Tomsick³, J. Lazendic⁴, A.K. Tzioumis⁵, Y. Butt⁶, R. Wijnands⁷

ABSTRACT

We report on new X-ray observations of the large-scale jets recently discovered in X-rays from the black hole candidate 4U 1755-33. Our observations in 2004 show that the jets found in 2001 are still present in X-rays. However, sensitive radio observations in 2004 failed to detect the jets. We suggest that synchrotron radiation is a viable emission mechanism for the jets and that thermal bremsstrahlung and inverse-Compton emission are unlikely on energetic grounds. In the synchrotron interpretation, the production of X-rays requires acceleration of electrons up to ~ 60 TeV, the jet power is $\sim 4 \times 10^{35}$ erg s⁻¹, and the radio non-detection requires a spectral index $\alpha > -0.65$ ($S_\nu \propto \nu^\alpha$) which is similar to the indexes found in lobes surrounding some other compact objects. We find an upper limit on the flux of 4U 1755-33 in quiescence of 5×10^{-16} erg cm⁻² s⁻¹ in the 0.3-8 keV band.

Subject headings: black hole physics: general – stars: black holes – stars: individual (4U 1755-33) – stars: winds, outflows – X-rays: binaries

1. Introduction

Relativistic jets are often produced by accreting compact objects, including both stellar-mass X-ray binaries and active galactic nuclei. Jets appear to be important in the dynamics of the overall accretion flow in such systems and a substantial fraction of the accretion energy of X-ray binaries may be dissipated in jets. Understanding the properties and production of jets is important for

our understanding of the energetics and dynamics of the accretion process. Further, the jets from X-ray binaries in the Milky Way are a potentially significant source of energy input to the Galactic ISM and, if hadronic, a likely source of cosmic rays (Heinz & Sunyaev 2002) and a possible source of Galactic light element nucleosynthesis (Butt et al. 2003).

Recent XMM-Newton observations have led to the discovery of a large scale X-ray jet from the long-term X-ray transient and black hole candidate 4U 1755–33 (Angelini & White 2003). The X-ray source 4U 1755–33 was discovered with Uhuru (Jones 1977) and was, therefore, active in 1970 and may have been active earlier. It was later found to have an unusually soft spectrum (White & Marshall 1984; White et al. 1984) and a hard X-ray tail (Pan et al. 1995) suggesting a black hole candidate. The source shows X-rays dips which indicate that the system has a high inclination and an orbital period of 4.4 days (White et al. 1984; Mason, Parmar, & White 1985). The source was still active in 1993 (Church & Balucinska-Church 1984), and then found in quiescence in 1996 (Roberts et al. 1996). The source was active

¹Department of Physics and Astronomy, University of Iowa, Van Allen Hall, Iowa City, IA 52242, USA; philip-kaaret@uiowa.edu

²AIM - Unité Mixte de Recherche CEA - CNRS - Université Paris VII - UMR 7158, CEA Saclay, Service d'Astrophysique, F-91191 Gif sur Yvette, France

³Center for Astrophysics and Space Sciences, University of California at San Diego, La Jolla, CA 92093-0424, USA

⁴Kavli Institute for Astrophysics and Space Research, Massachusetts Institute of Technology, 77 Massachusetts Avenue, Cambridge, MA 02139

⁵Australia Telescope National Facility, CSIRO, P.O. Box 76, Epping, NSW 1710, Australia

⁶Harvard-Smithsonian Center for Astrophysics, 60 Garden St., Cambridge, MA 02138, USA

⁷Astronomical Institute 'Anton Pannekoek', University of Amsterdam, Kruislaan 403, 1098 SJ Amsterdam, The Netherlands

for at least 23 years. The distance to the source is poorly constrained. It is likely greater than 4 kpc because the optical counterpart (identified during outburst; McClintock, Canizares, & Hiltner 1978) was not detected in quiescence (Wachter & Smale 1998), but less than 9 kpc because of the low level of visual extinction (Mason, Parmar, & White 1985).

Angelini & White (2003) found a linear X-ray structure which is roughly symmetric about the position of 4U 1755–33 extending about 3′ to the north-west and 3′ to the south-east of the black hole candidate. There appear to be multiple knots in the jets. For estimated distances of 4–9 kpc, the angular size corresponds to jet lengths of 3–8 pc. Therefore, the jet must have taken at least 10–30 years to form. The source was active for at least 23 years which appears sufficient to have formed the jet. Chandra observations do not show point sources along the jet, but do give a detection of emission over the area of the jet (Park et al. 2005). This indicates that the jet emission seen with XMM-Newton is truly diffuse and not an alignment of point sources.

The primary questions concerning the jet are: what is the X-ray emission mechanism, how is the jet powered, and what is the total energy in the jet? We obtained new observations of 4U 1755–33 using XMM-Newton and the Australia Telescope Compact Array (ATCA) to attempt to measure a multiwavelength spectrum and observe the evolution of the jet. We describe the X-ray observations and analysis in §2, the radio observations and analysis in §3, and draw conclusions regarding the properties of the jet in §4.

2. XMM-Newton Observations and Analysis

We observed 4U 1755–33 using XMM-Newton beginning on 18 Sep 2004 for 45.9 ks (Observation identifier 0203750101). We refer to this observation as “B”. We also analyzed an archival observation obtained by Angelini & White (2003) beginning on 8 Mar 2001 with a duration of 19.4 ks (Observation identifier 0032940101). We refer to this observation as “A”. Our observation was designed to have the same pointing and instrument modes as the earlier observation in order to facilitate comparison. The EPIC detectors were oper-

ated in full frame mode so that a large field could be imaged.

We reduced the data using the standard procedures described in the XMM-Newton User’s Handbook and the XMM-Newton ABC Guide. We used SAS version 6.1.0. Calibration files were obtained using the online version of *cifbuild* available at XMM-Newton Science Operations Centre home page (<http://xmm.vilspa.esa.es>) on 11 Jan 2005. There were no obvious background flares in observation A and only a few small flares of less than 15% of the total count rate in observation B, so we decided not to filter the events on count rate as is often necessary to remove background flares. In our analysis, we used only the EPIC MOS detectors because there are sizable chip gaps in the PN in the region covered by the jet. We extracted single, double, and triple events (PATTERN \leq 12) for the MOS data and filtered according standard procedures to eliminate events in bad pixels or rows or frames, in flickering pixels, identified as cosmic-rays, outside the pulse height thresholds, near the CCD boundary, or outside the nominal field of view (specifically, we required FLAG equal to #XMMEA_EM).

2.1. Point sources

We created images in sky coordinates in the 0.3–10 keV band and used *edetect_chain* to search for sources in the two MOS images for each observation. Our primary interest in source detection is the alignment of the two images, so we considered only sources with very high significance (likelihood parameter \geq 50, equivalent to a single trial significance of 17σ) because these sources give the most accurate positions. A list of high significance sources is presented in Table 1. Many sources of lower significance are present in the images. The fluxes are for the 0.3–10 keV band and calculated from the count rate in this band assuming a power-law spectrum with a photon index of 1.5 and interstellar absorption with $N_H = 3.1 \times 10^{21} \text{ cm}^{-2}$ equal to the hydrogen column density along the line of sight in the Milky Way.

We searched for spatial coincidences between the source list from observation B and the catalog of 2mass point sources. The astrometric accuracy of sources in the 2mass catalog is 0.2″. We considered only sources with J magnitudes brighter than 12.5 to limit the source density. We find

TABLE 1
XMM-NEWTON X-RAY SOURCES NEAR 4U 1755-33

	RA	DEC	Error	Flux A	Flux B	Counterparts
1	17 59 00.86	-33 45 48.1	0.2	243.9 ± 10.0	171.9 ± 4.0	AW2003 1, 2mass
2	17 57 58.88	-33 46 24.9	0.4	218.4 ± 12.1	45.1 ± 2.7	2mass
3	17 59 21.83	-33 53 15.6	0.7	77.1 ± 7.1	14.9 ± 1.9	AW2003 3
4	17 58 26.89	-33 59 53.8	0.8	76.2 ± 9.7	-	
5	17 58 42.02	-33 41 48.8	0.3	29.3 ± 3.8	71.6 ± 2.9	1WGA J1758.6-3341
6	17 59 22.79	-33 50 25.2	0.7	63.8 ± 7.0	24.4 ± 2.3	1WGA J1759.3-3350, 2mass
7	17 58 20.25	-33 42 51.8	0.6	63.4 ± 7.7	33.7 ± 2.2	
8	17 58 49.48	-33 41 40.8	0.5	56.6 ± 5.7	42.7 ± 2.7	2mass
9	17 58 36.67	-33 40 27.3	0.6	-	55.0 ± 5.7	
10	17 58 38.88	-33 57 00.3	0.4	-	49.0 ± 2.5	
11	17 58 21.03	-33 46 54.7	0.3	34.1 ± 4.3	41.8 ± 1.9	2mass
12	17 59 27.97	-33 49 10.3	1.5	37.0 ± 4.5	-	
13	17 58 44.04	-33 46 13.0	0.5	29.2 ± 3.4	11.7 ± 1.2	
14	17 57 40.65	-33 45 53.9	0.6	-	25.4 ± 2.3	
15	17 58 59.19	-33 50 16.3	0.5	25.3 ± 3.2	20.4 ± 1.5	
16	17 58 44.16	-33 45 09.5	0.6	24.5 ± 3.2	12.2 ± 1.4	
17	17 59 03.24	-33 59 18.1	0.9	-	17.8 ± 2.2	
18	17 58 51.23	-33 49 13.8	0.7	-	17.1 ± 1.4	
19	17 58 25.56	-33 57 46.8	2.8	-	15.8 ± 1.7	
20	17 58 24.23	-33 52 58.8	0.5	-	14.8 ± 1.3	
21	17 58 49.58	-33 57 14.0	0.6	-	14.1 ± 1.6	2mass
22	17 58 12.44	-33 43 56.6	0.9	-	14.0 ± 1.7	
23	17 58 14.22	-33 49 08.7	0.8	-	11.7 ± 1.2	
24	17 58 43.37	-33 58 17.8	1.0	-	11.6 ± 1.5	
25	17 59 08.17	-33 46 47.7	0.7	-	9.5 ± 1.3	
26	17 58 46.92	-33 48 44.7	1.0	-	8.0 ± 1.1	
27	17 58 22.29	-33 47 43.7	1.0	-	7.9 ± 1.0	

NOTE.—Table 1 includes for each source: the source number; RA and DEC – the position of the source in J2000 coordinates; Error – the statistical error on the source position in arcseconds, note that this does not include errors in the overall astrometry; Flux A – the source flux for observation A in units of 10^{-14} erg cm $^{-2}$ s $^{-1}$ in the 0.3–10 keV band calculated assuming a power law spectrum with photon index of 1.5 and corrected for the Galactic absorption column density of 3.1×10^{21} cm $^{-2}$; Flux B – the same for observation B; Counterparts – indicates counterparts in Angelini & White (2003) (AW2003), the 2Mass catalog (2mass), or the WGA catalog (WGA).

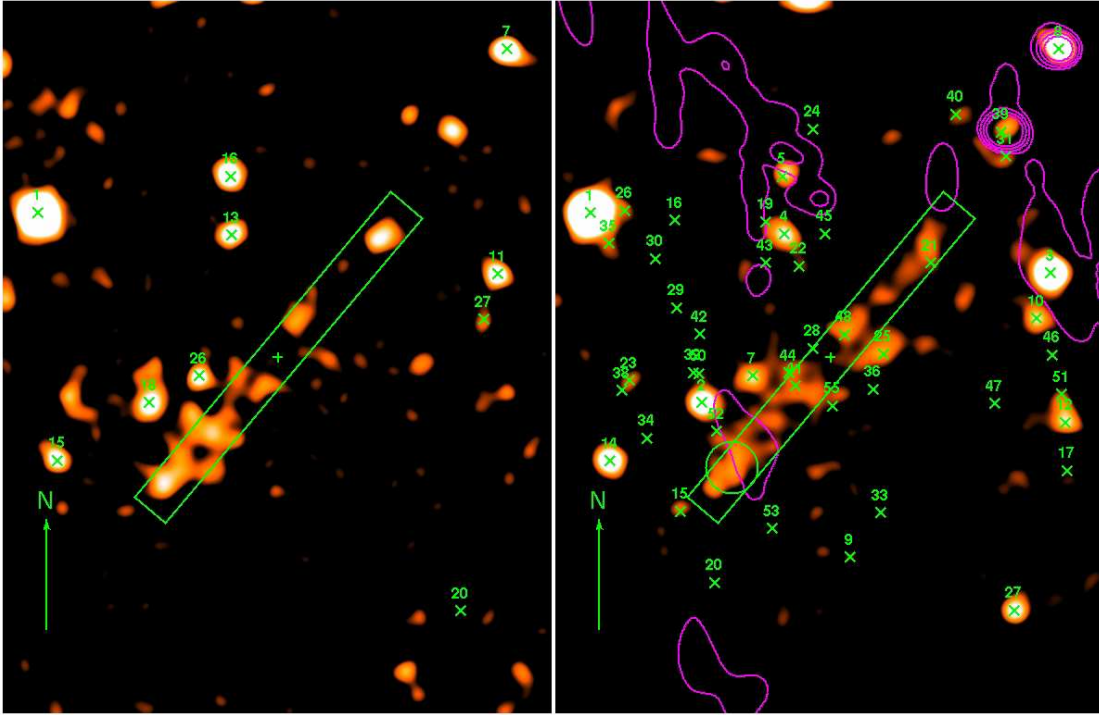


Fig. 1.— XMM-Newton images of 4U 1755–33. The image on the left is observation A (8 Mar 2001) on the right is observation B (18 Sep 2004). The green cross indicates the position of 4U 1755–33. The green rectangle encloses the jet and has a size of $44''$ by $430''$. On the left image, the green X’s mark the positions of XMM-Newton point sources reported in Table 1. On the right image, the green X’s mark the positions of Chandra point sources reported in Table 3. The green arrow indicates North and is $2'$ long. Radio contours are superimposed on the image on the right in magenta. The radio contours represent the flux density at 13 cm at levels of 0.3, 0.6, 1.2, and 2.4 mJy. Also, on the right image, the green circle indicates the extraction region used to find the spectrum of the jet bright spot described in the text.

1290 sources within $10'$ of 4U 1755–33 for a source density of $0.0011 \text{ arcsec}^{-2}$. There are 4 matches between X-ray and 2mass sources within $0.9''$ and one additional match with an offset of $1.1''$. Given the source density quoted above, the probability of a chance coincidence within $0.9''$ between a 2mass source and a given X-ray source is 0.3%. We conclude that the absolute astrometry of the XMM image is good to within $1.0''$. We aligned observation A to observation B by matching 11 sources detected in both observations. The needed shift was $0.15''$ in RA and $1.3''$ in DEC. After the shift, the average magnitude of offset in source positions between the two observations is $1.4''$ which is about twice the typical statistical uncertainty in the positions as calculated by the SAS routine *emldetect*. We take $1.4''$ as an estimate of the typical

uncertainty in the relative XMM-Newton source positions between the two observations. Adding in the uncertainty in the absolute astrometry, we estimate the typical total uncertainty in the XMM Newton source positions as $1.7''$.

2.2. Jet morphology

Images of the region around 4U 1755–33 are shown in Fig. 1. The images are for the 0.3–10 keV band. Each image is the summed MOS1+MOS2 data in the 0.3–10 keV band and has been smoothed with a gaussian filter with $\sigma = 8''$. The jet extends to the NW (up and to the right) and SE (down and to the left) from 4U 1755–33. The positions of point sources reported in Table 1 are marked on the image. Note that the image shown covers only a portion of the field of view, so

several sources listed in the Tables are not present on the image.

Fig. 2 shows the profiles of counts along the jet axis. The numbers of counts for observation A were multiplied by a factor of 2.51 to compensate for the shorter exposure time. Each profile represents the counts in the 0.5-10 keV band integrated in bins which extend $2''$ along the jet axis and have a full width of $44''$ perpendicular to the jet axis (the width is the same as the rectangular region shown in Fig. 1). The profiles were smoothed with a gaussian with $\sigma = 6''$.

The morphology of the jet appears similar in the two observations. There appears to be some correspondence between knots found in the two observations, but extraction of knot motions is ambiguous because the morphologies of the individual knots have changed. With this caveat, we consider the morphology of the jet close to 4U 1755–33. Assuming that the black hole candidate (BHC) is no longer feeding the jet, one might expect the gap around the BHC to widen if the jets are moving away from the BHC. The knot to the SW closest to the BHC (at a displacement of $-30''$ in Fig. 2) does appear to have shifted away from the BHC by $12''$ if we compare the peaks of the two profiles in Fig. 2. This corresponds to a speed of $\sim 0.2c$ for a distance of 4 kpc ($\sim 0.4c$ for 9 kpc). However, on the NE side of the jet, the closest knot appears to have remained stationary. We stress that any conclusions regarding physical motion of the jets is ambiguous. In particular, it is unclear if these changes are really secular or merely random changes of flux over time, perhaps associated with interactions of the jet with the ISM.

2.3. Jet spectrum and evolution

We extracted spectra of the jet emission for each observation using the rectangular regions shown in Fig. 1. Background spectra were extracted from a region with identical size and orientation displaced to a source-free region to the Southwest of the jet. We used both MOS cameras for each observation and fit the two MOS spectra simultaneously using *XSPEC* 11.3.1.

We found adequate fits to the spectra with a power-law subject to interstellar absorption and with a MEKAL thermal plasma emission model with solar abundances, again, subject to interstel-

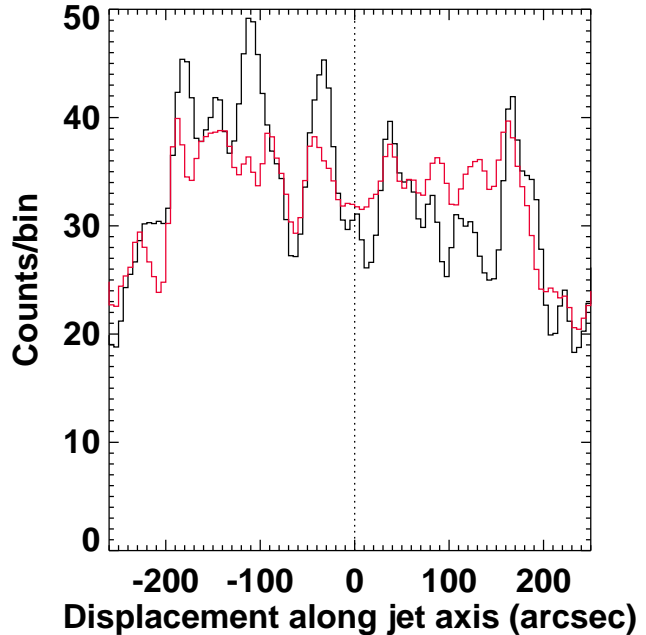


Fig. 2.— Profile of counts along the jet. The black line is observation A and the red line is for observation B. The counts for observation A were multiplied by a factor a 2.51 to compensate for the shorter observation time of that observation. The dotted line marks the position of 4U 1755-33.

lar absorption, see Fig. 3. The fit results are presented in Table 2. We performed fits both with the interstellar absorption hydrogen column density, N_H , fixed to the value found along the line of sight in HI maps (Dickey & Lockman 1990) and also allowing N_H to vary. We used the absorption model of Wilms, Allen, & McCray (2000) which is *tbabs* in *XSPEC*. We calculated the errors on the parameters using $\Delta\chi^2 = 2.71$ corresponding to 90% confidence for one free parameter of interest for the fits with N_H fixed, and $\Delta\chi^2 = 4.61$ corresponding to 90% confidence for two free parameters of interest for the fits with N_H allowed to vary. In the table, we report both the observed flux in the 0.5-10 keV band and the flux corrected for the effects of interstellar absorption.

Both the power-law and the MEKAL thermal plasma model provide adequate fits to the spectra. Allowing N_H to be a free parameter widens the allowed ranges of the fit parameters. The preferred values for N_H , when free, tend to be below the column density along the line of sight toward the

TABLE 2
X-RAY SPECTRAL FITS TO JET EMISSION

Model	N_H	Γ/kT	χ^2/DoF	Flux	Unabsorbed Flux
Observation A: 8-Mar-2001					
Power-law	3.1	1.7 ± 0.3	19.3/20	2.0	2.5
Power-law	$2.4^{+2.1}_{-1.3}$	1.6 ± 0.4	18.8/19	2.1	2.5
MEKAL	3.1	> 3.7	22.5/20	1.9	2.4
MEKAL	$1.4^{+2.4}_{-1.3}$	> 4.5	20.3/19	2.1	2.3
Observation B: 18-Sep-2004					
Power-law	3.1	1.5 ± 0.3	13.9/20	1.6	1.9
Power-law	$1.9^{+1.9}_{-1.3}$	1.4 ± 0.4	12.5/19	1.7	1.9
MEKAL	3.1	> 5.2	13.8/20	1.6	1.9
MEKAL	$1.8^{+1.7}_{-1.3}$	> 6.1	12.2/19	1.7	1.8

NOTE.—Table 2 includes for each spectral model: Model - the model name (note all models include photoelectric absorption); N_H - the column density for photoelectric absorption in units of 10^{21} cm^{-2} ; Γ/kT - the photon index Γ for power-law models or the temperature kT in keV for MEKAL models; χ^2/DoF - the χ^2 and the number of degrees of freedom; Flux - the source flux in units of $10^{-13} \text{ erg cm}^{-2} \text{ s}^{-1}$ in the 0.5–10 keV band; Unabsorbed Flux - the source flux in units of $10^{-13} \text{ erg cm}^{-2} \text{ s}^{-1}$ in the 0.5–10 keV band corrected for interstellar absorption.

source, but include the line of sight density within the error interval.

No line emission is apparent. The upper bounds on line emission depend on the assumed line parameters. For line parameters similar to those found for SS433 (Watson et al. 1986), we find 90% confidence upper bounds on the equivalent widths of Fe-K emission lines of 0.6–2 keV. These are in the range of the equivalent width measured for the inner jets of SS433 (Migliari et al. 2002) and are not constraining.

We also fit a spectrum for a region enclosing a bright spot toward the SE end of the jet for observation B. The region is shown in Fig. 1 and has radii of $28''$. This radius was selected to allow comparison with the radio beam, discussed below. The region was located to maximize the X-ray flux within that radius. We find an adequate fit with an absorbed power-law model with the absorption column density fixed to $N_H = 3.1 \times 10^{21} \text{ cm}^{-2}$. We find a photon index $\Gamma = 1.78 \pm 0.52$, a flux of $2.8 \times 10^{-14} \text{ erg cm}^{-2} \text{ s}^{-1}$ in the 0.5–10 keV band, and a flux corrected for absorption of $3.6 \times 10^{-14} \text{ erg cm}^{-2} \text{ s}^{-1}$.

From our two observations, we can make a crude estimate of the decay time of the jet. To minimize the dependence on the fitted spectral model, we re-fitted the data using a power-law model with the photon index fixed to 1.73 (the

best fit value for observation A) with interstellar absorption with $N_H = 3.1 \times 10^{21} \text{ cm}^{-2}$. Adequate fits were found in all cases. We repeated the same procedure using a MEKAL model with fixed parameters and find that the fluxes differ by less than 5%. The uncertainty in the flux measurement is dominated by the uncertainty in the background subtraction. We find fluxes of $(20.0 \pm 2.2) \times 10^{-14} \text{ erg cm}^{-2} \text{ s}^{-1}$ in the 0.5–10 keV band for observation A and $(14.6 \pm 1.4) \times 10^{-13} \text{ erg cm}^{-2} \text{ s}^{-1}$ for observation B. For an exponential decay, the $1/e$ folding time is 11^{+24}_{-4} years. We also considered the evolution of the Northern and Southern halves of the jet independently. For the Southern half of the jet, the flux is $(12.5 \pm 1.7) \times 10^{-14} \text{ erg cm}^{-2} \text{ s}^{-1}$ in the 0.5–10 keV band for observation A and $(7.8 \pm 1.0) \times 10^{-13} \text{ erg cm}^{-2} \text{ s}^{-1}$ for observation B. The $1/e$ folding time of is $7.6^{+2.2}_{-1.3}$ years. The flux from the Northern part of the jet in observation B is consistent within the uncertainties with that in observation A. Therefore, we can place only a lower bound on the decay time of the Northern jet of 8 years.

3. Radio Observations and Analysis

On 27 April 2004, we obtained continuum radio observations of 4U 1755–33 using the Australia Telescope Compact Array (ATCA) located in Narrabri, New South Wales, Australia. This is

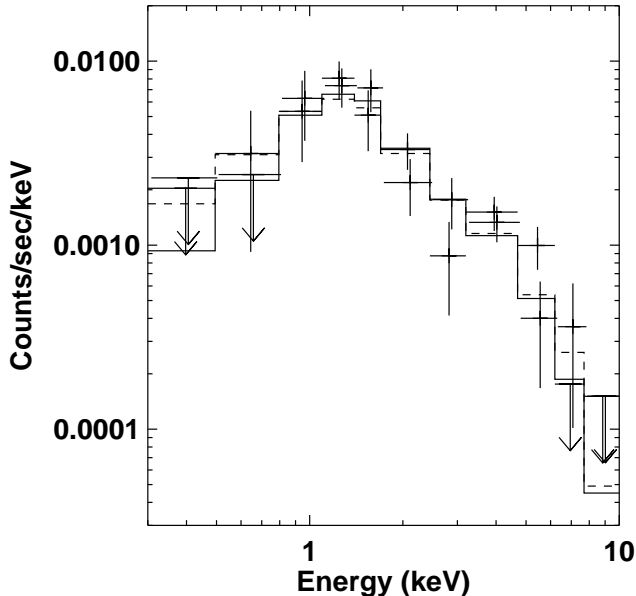


Fig. 3.— X-ray spectrum of jet emission for observation A. The data from the two MOS units are shown. The energy bins for MOS2 are artificially shifted up by 2% for clarity. The fit of a power-law model with absorption with $N_H = 3.1 \times 10^{21} \text{ cm}^{-2}$ is shown as a solid line. The fit of a mekal model with the same absorption is shown as a dashed line.

153 days before our XMM-Newton observations, but still reasonably contemporaneous given the long life-time of the jet. The ATCA synthesis telescope consists of five 22 m antennas, which can be positioned along an east-west track with a short north-south spur, and a sixth antenna at a fixed location. The ATCA uses orthogonal polarized feeds and records full Stokes parameters. We observed with the ATCA for 10 hours at 1384 MHz (21.7 cm) and 2368 MHz (12.7 cm) simultaneously, with the array in the EW367 compact configuration which has baselines ranging from 46 to 4408 m. Because an interferometer acts as a filter for low spatial scales, the maximum angular size that can be imaged with the ATCA in this configuration is of the order of $5'$ at 2368 MHz ($8'$ at 1384 MHz). Since the X-ray jets in 4U 1755–33 are diffuse hot spots, rather than a continuous smooth structure, radio imaging of the jets is possible with this ATCA configuration. The amplitude and band-pass calibrator was PKS 1934–638,

and the antenna’s gain and phase calibration, as well as the polarization leakage, were derived from regular observations of the nearby (6° away) calibrator PMN 1729–37. The editing, calibration, Fourier transformation, deconvolution, and image analysis were performed using the MIRIAD software package (Sault & Killeen 1998).

An image of the radio emission at 2.4 GHz (13 cm) is shown as contours in the right panel of Fig. 1. Strong radio sources were detected in the northwest region of the field, but there is no significant detection of emission over the region of the X-ray jet. The rms sensitivity is 0.2 mJy/beam. There is a slight hint of emission toward the SE end of the jet, but the flux density is always below 0.6 mJy and does not constitute a detection. The image at 1.4 GHz also shows no evidence for a significant detection of emission over the area of the jet.

TABLE 3
CHANDRA X-RAY SOURCES NEAR 4U 1755-33

No.	RA	DEC	Error	Flux 2003	Flux 2004	Counterparts
1	17 59 00.859	-33 45 48.67	0.1		168 ± 7	[AW2003] 1, 2mass
2	17 58 51.181	-33 49 13.96	0.1	57 ± 6	43 ± 4	XMM 18
3	17 58 21.041	-33 46 53.66	0.1	64 ± 6	169 ± 9	XMM 11
4	17 58 44.051	-33 46 12.00	0.1	34 ± 5	47 ± 4	XMM 13
5	17 58 44.259	-33 45 09.68	0.1	47 ± 5	33 ± 3	XMM 16
6	17 57 58.976	-33 46 25.94	0.1		217 ± 12	XMM 2
7	17 58 46.824	-33 48 45.02	0.1	26 ± 4	19 ± 2	XMM 26
8	17 58 20.343	-33 42 51.82	0.1	171 ± 16	98 ± 7	XMM 7
9	17 58 38.416	-33 52 00.99	0.3	10 ± 3	19 ± 2	
10	17 58 22.234	-33 47 42.75	0.2	41 ± 5	26 ± 3	XMM 27
11	17 58 12.455	-33 43 56.47	0.2		44 ± 6	XMM 22
12	17 58 19.725	-33 49 35.24	0.2		21 ± 3	
13	17 58 38.734	-33 57 00.24	0.1	57 ± 9		
14	17 58 59.146	-33 50 16.97	0.2	22 ± 4		
15	17 58 53.104	-33 51 11.25	0.2	11 ± 3	7.0 ± 1.5	
16	17 58 53.508	-33 45 56.84	0.2		9.9 ± 1.8	
17	17 58 19.579	-33 50 27.36	0.2		14 ± 2	
18	17 58 05.137	-33 46 07.22	0.2		26 ± 4	
19	17 58 45.698	-33 45 58.70	0.2		8.4 ± 1.7	
20	17 58 50.079	-33 52 28.71	0.2		6.7 ± 1.5	
21	17 58 31.416	-33 46 42.77	0.3	12 ± 3		
22	17 58 42.817	-33 46 46.27	0.1		5.6 ± 1.3	
23	17 58 57.504	-33 48 49.89	0.2		5.3 ± 1.3	
24	17 58 41.580	-33 44 18.61	0.2	13 ± 4		
25	17 58 35.470	-33 48 21.62	0.2	5.8 ± 1.9	6.4 ± 1.4	
26	17 58 57.877	-33 45 46.42	0.1	15 ± 3	5.2 ± 1.4	XMM 22
27	17 58 24.178	-33 52 58.22	0.1	13 ± 4		
28	17 58 41.560	-33 48 15.43	0.2		4.3 ± 1.2	
29	17 58 53.396	-33 47 31.43	0.1	8 ± 2	4.3 ± 1.2	
30	17 58 55.258	-33 46 38.68	0.3		3.7 ± 1.1	2mass
31	17 58 24.932	-33 44 47.96	0.2		14 ± 3	
32	17 58 51.943	-33 48 41.59	0.1		3.7 ± 1.1	
33	17 58 35.714	-33 51 13.17	0.2		4.6 ± 1.3	
34	17 58 55.982	-33 49 52.40	0.2		4.5 ± 1.2	
35	17 58 59.228	-33 46 22.15	0.2		3.6 ± 1.2	
36	17 58 36.358	-33 48 59.51	0.2	5.7 ± 1.9	4.0 ± 1.2	2mass
37	17 57 53.117	-33 47 01.93	0.2		8 ± 7	
38	17 58 58.107	-33 49 00.99	0.2		2.9 ± 1.0	
39	17 58 25.308	-33 44 21.14	0.1	12 ± 4	20 ± 5	
40	17 58 29.228	-33 44 02.49	0.2	8 ± 3	10 ± 2	
41	17 58 43.075	-33 48 56.07	0.3		3.1 ± 1.0	
42	17 58 51.382	-33 47 59.83	0.3	8 ± 2		
43	17 58 45.690	-33 46 42.96	0.1		5.1 ± 1.2	
44	17 58 43.694	-33 48 42.10	0.3		2.9 ± 1.0	
45	17 58 40.548	-33 46 11.34	0.2		5.2 ± 1.4	
46	17 58 20.885	-33 48 22.09	0.3		6.0 ± 1.6	
47	17 58 25.897	-33 49 14.88	0.4		4.8 ± 1.5	
48	17 58 38.894	-33 48 00.68	0.3		3.3 ± 1.0	
49	17 58 49.783	-33 58 21.79	0.2	27 ± 7		
50	17 58 51.420	-33 48 42.47	0.3		3.1 ± 1.0	2mass
51	17 58 20.112	-33 49 04.92	0.3	19 ± 5	6 ± 2	
52	17 58 49.906	-33 49 44.76	0.2		2.8 ± 0.9	
53	17 58 45.112	-33 51 29.75	0.3		3.1 ± 1.0	
54	17 58 42.143	-33 55 58.54	0.2	9 ± 3		
55	17 58 39.876	-33 49 17.69	0.6	4.8 ± 1.8		
56	17 58 11.545	-33 45 02.64	0.4		6 ± 3	

NOTE.—Table 3 includes for each source: the source number; RA and DEC – the position of the source in J2000 coordinates; Error - the statistical error on the source position in arcseconds,

note that this does not include errors in the overall astrometry; Flux 2003 – the source flux on 25 Sept 2003 in units of 10^{-15} erg cm $^{-2}$ s $^{-1}$ in the 0.3–10 keV band calculated assuming a power law spectrum with photon index of 1.5 and corrected for the Galactic absorption column density of 3.1×10^{21} cm $^{-2}$; Flux 2005 – the source flux on 25 June 2004; Counterparts - indicates counterparts in Angelini & White (2003) (AW2003), the 2Mass catalog (2mass), or the XMM sources in Table 1 (XMM).

4. Chandra Observations and Analysis

To determine if the features found in the XMM-Newton X-ray image are point sources or truly diffuse emission, we analyzed two Chandra observations obtained of the same field. The observations are a 22 ks exposure obtained on 25 Sept 2003 (ObsID 3510, PI S. Murray) and a 45 ks exposure obtained on 25 June 2004 (ObsID 4586, PI L. Angelini). The 2003 observation is the one analyzed by Park et al. (2005).

The Chandra data were subjected to the usual data processing and event screening and analyzed using the *CIAO* version 3.1 data analysis package, e.g. Kaaret (2005). We constructed images using all valid events on the S2 and S3 chips for ObsID 3510 and all events on the S3 and S4 chips for ObsID 4586. We computed exposure maps for each image for a power-law spectrum with photon index of 1.5 absorbed by a column density of $N_H = 3.1 \times 10^{21} \text{ cm}^{-2}$. We used the *wavdetect* tool to search for X-ray sources. The sources with detection significance of 4σ or higher are listed in Table 3.

We aligned the Chandra observations with sources in the 2mass point source catalog, as done for the XMM-Newton image above. We restricted the sources to have J magnitudes brighter than 12.5 to limit the source density. After applying a shift of $0.3''$ to the Chandra astrometry, there are 4 matches within $0.2''$ between Chandra sources in ObsID 4586 and 2mass sources. We conclude that our corrected Chandra astrometry for ObsID 4586 is good to within $0.2''$. We aligned ObsID 3510 to ObsID 4586 using several X-ray sources present in both images.

Summing the flux from all of the sources within the jet, as defined by the region shown in Fig. 1, we find that discrete point sources contribute less than 10% of the total jet flux in each observation. Hence, we confirm the results of Park et al. (2005) that the X-ray jet from 4U 1755–33 is truly diffuse. We note that there are Chandra point source counterparts to the two radio sources beyond the jet to the northwest. Therefore, these two radio sources are not associated with the diffuse X-ray emission of the jet.

To investigate the flux from 4U 1755–33 itself, we extracted counts from a circular region with a radius of $2''$ at the position of the op-

tical counterpart. We find a total of 3 counts in the 0.3–8 keV band in the two images. Using a $15''$ radius region, we estimated the background in the source extraction region to be 3.0 counts. Therefore, we detect zero net counts from 4U 1755–33. Allowing for a Poisson distribution of counts, a 95% confidence upper limit on the number of source counts is 3.0. For a power-law spectrum with photon index of 1.5 absorbed by a column density of $N_H = 3.1 \times 10^{21} \text{ cm}^{-2}$, this corresponds to an upper limit on the source flux of $5 \times 10^{-16} \text{ erg cm}^{-2} \text{ s}^{-1}$. The upper limit on the unabsorbed flux is $6 \times 10^{-16} \text{ erg cm}^{-2} \text{ s}^{-1}$. For distances of 4–9 kpc, this corresponds to a limit on the luminosity of $1 - 6 \times 10^{30} \text{ erg s}^{-1}$. This is similar to the quiescent luminosities of other short orbital period black hole X-ray binaries such as XTE J1118+480 and A 0620-00 (Corbel, Tomsick, & Kaaret 2005).

5. Discussion

There is now known to exist a broad range of jets from stellar-mass X-ray binaries. Persistent compact jets with lengths of tens of A.U. are produced in the low/hard X-ray spectral state. Impulsive jets produced at state transitions have been detected on lengths scales from hundreds of A.U. out to parsecs. Stationary lobes have been found in the radio at separations of several parsecs for sources such as 1E1740.7-2942 and GRS 1758-258 and in the X-ray with separations up to 70 pc from SS 433 (Watson et al. 1983).

The jet size of 3–8 pc in 4U 1755–33 is larger than the transient large-scale moving jets of XTE J1550-564 (Corbel et al. 2002) and H 1743–322 (Corbel et al. 2005), but is similar to the total size of the stationary radio lobes of 1E1740.7-2942 and GRS 1758-258 (Mirabel & Rodríguez 1999). The latter two sources are persistent X-ray emitters, similar in properties to 4U 1755–33 while it was X-ray bright. This may suggest that 4U 1755–33 represents the formation of a large-scale, nearly stationary jet.

The central source in 4U 1755–33 has turned off and we now see the decay of the jet over a time scale of 10–40 years or perhaps longer for the Northern part of the jet. While we can place only a lower bound of 23 years on the time over which the central source was active, and the jet was be-

ing energized, our detection of the decay of the jet suggests that the time scale for the energization of the jet is similar to or shorter than the decay time. We note that we detect flux decay only for the southern jet. The change in morphology is also stronger for the inner regions of the southern jet. This may suggest that the southern jet is the approaching and the northern jet is receding. Continued monitoring of 4U 1755–33 may reveal motion and decay of the northern jet.

A key question is the nature of the jet emission. We consider three possible emission mechanisms: thermal bremsstrahlung, inverse-Compton, and synchrotron.

If the X-ray emission is thermal bremsstrahlung, then the total mass and energy of the jet can be estimated from its observed luminosity, temperature, and volume. For the volume, we assume that the jet occupies a roughly cylindrical volume with a diameter perpendicular to the direction of motion of $0.2'$ and a linear dimension of $6'$ multiplied by a filling factor of 0.2. The volume is then $2 \times 10^{54} \text{ cm}^3$ for an assumed distance of 4 kpc. We took the flux from the X-ray spectral fits, and set $kT = 5 \text{ keV}$ which is the minimum temperature consistent with the fits. We find that the density of the jet material is 4 cm^{-3} , the total energy of the jet is $2 \times 10^{47} \text{ erg}$ and the total mass in the jet is $1 \times 10^{31} \text{ g}$. The cooling time of the gas would then be $6 \times 10^6 \text{ yr}$ which is much longer than the observed decay time. Also, if the jet were fed by the outflow from a mass accretion rate of 10^{19} g/s corresponding the Eddington rate for a $10M_{\odot}$ compact object, at least 10^4 years would be required to accumulate the needed mass. This is much longer than the observed decay time scale and we conclude that the jet emission is unlikely to be thermal bremsstrahlung.

The best candidate source of seed photons for inverse-Compton scattering is the interstellar radiation field (ISRF). The ISRF varies strongly with Galactocentric radius and height above the Galactic plane. On the sky, 4U 1755–33 is rather close to the Galactic center and it could be physically close to the Galactic center, although the low optical extinction suggests that the source is actually nearer than the Galactic bulge. We assume that 4U 1755–33 is at a distance of 8.5 kpc, close to the Galactic center, which maximizes the ISRF energy density. We adopt an energy density of 10 eV cm^{-3} , equal

to the maximum found anywhere in the Milky Way (Strong, Moskalenko, Reimer 2000) and assume, for simplicity, that all of the radiation is in the dominant component of ISRF near $1 \mu\text{m}$ (Mathis, Mezger, & Panagia 1983). To produce X-rays in the 0.3–10 keV, electrons with energies from ~ 5 to $\sim 100 \text{ MeV}$ are required. For an assumed X-ray spectral index $\alpha = -0.5$, defined as $S(\nu) \propto \nu^{\alpha}$, the total energy in relativistic electrons required is $\sim 10^{50} \text{ erg}$. A $10M_{\odot}$ black hole producing energy at the Eddington rate with all of the energy going to perfectly efficient acceleration of electrons in the desired energy range would require ~ 2000 years to power the jet. This is much longer than the observed decay time scale. Therefore, it appears unlikely that the jet emits via inverse-Compton radiation.

If X-ray emission is synchrotron, then synchrotron radio emission should be expected. To determine if our upper limits on the radio flux are consistent with synchrotron emission, we consider the emission from the brightest X-ray spot along the jet. The X-ray spectrum was extracted from a circle with a radius of $28''$. This is slightly larger than the radio beam size at 2.4 GHz, so we can compare the X-ray flux density in the regions to the radio upper limit per beam, which we take as 3 times the rms noise level of 0.2 mJy. Comparing the X-ray and radio flux density, we derive a lower limit on the radio/X-ray spectral index $\alpha > -0.65$, i.e. the spectrum must be flatter than $\alpha = -0.65$. Therefore, our radio observations may simply be not sensitive enough to detect the radio synchrotron emission. The limit on the spectral index implies that the exponent, p , of the electron energy distribution, $N(E) \propto E^{-p}$, must be $p < 2.3$. This is within the range that can be produced by relativistic shocks. The spectral index is similar to that measured for the large-scale jets of the black hole candidate X-ray transient XTE J1550–564 of $\alpha = -0.660 \pm 0.005$ (Corbel et al. 2002) and consistent with the index of $\alpha = -0.45$ measured for the eastern lobe of SS 433 (Safi-Harb & Petre 1999).

To investigate the energetics of a jet radiating via synchrotron emission, we calculate the equipartition magnetic field. Using a spectral index $\alpha = -0.6$ which is consistent with the bound above, a lower frequency cutoff of 2.4 GHz, and the same assumption for distance and volume as

for the thermal bremsstrahlung case, we find a magnetic field of $36 \mu\text{G}$. The electrons producing the X-ray emission must have Lorentz factors up to 6×10^7 , corresponding to energies of up to 60 TeV. The radiative lifetime of these electrons is of order 320 years. The minimum total energy required is 2×10^{44} erg and the number of electrons needed to produce the observed radiation is 1.2×10^{46} . Assuming that the jet is composed of normal matter (i.e. roughly one proton per electron), then the required mass is 2×10^{22} g. These numbers are relatively insensitive to distance. For a distance of 9 kpc, the magnetic field decreases to $29 \mu\text{G}$, the required energy increases to 1.5×10^{45} erg, and the required mass increases to 1.3×10^{23} g. For the larger distance, the energy required corresponds to 2 weeks accumulation at the Eddington rate for a $10 M_{\odot}$ black hole and the mass could be accumulated in less than one day. Thus, the energy and material required for a synchrotron emitting jet could easily have been accumulated over the 20 year active phase of the X-ray source. Using the decay rate calculated for the entire jet and the energy estimate from the synchrotron equipartition calculation, the energy loss rate is then $\sim 4 \times 10^{35} \text{ erg s}^{-1}$ for a 4 kpc distance. This is about 1% of the Eddington luminosity for a $10 M_{\odot}$ black hole and, therefore, the jet could have been energized by the conversion of a few percent of the energy into relativistic electrons.

The available data on the jet of 4U 1755–33 are consistent with the X-rays being synchrotron emission. Synchrotron emission also is the most favorable mechanism in terms of the required mass and energy. However, significantly deeper radio observations are required to test if the predicted synchrotron radio emission is produced.

We thank an anonymous referee for useful comments and the XMM-Newton team for successfully executing the observation. PK acknowledges partial support from NASA grant NNG05GA08G and a faculty scholar award from the University of Iowa. JAT acknowledges partial support from NASA grant NNG04GQ05G.

REFERENCES

Angelini, L. & White, N.E. 2003, *ApJ*, 586, L71

- Butt, Y. et al. 2003, 587, 748
- Church, M.J. & Balucinska-Church, M. 1997, *A&A*, 317, L47
- Corbel, S., Fender, R.P., Tzioumis, T., Tomsick, J.A., Orosz, J.A., Miller, J.M., Wijnands, R., & Kaaret, P. 2002, *Science*, 298, 196
- Corbel, S., Kaaret, P., Fender, R.P., Tzioumis, A.K., Tomsick, J.A., Orosz, J.A. 2005, *ApJ*, 632, 504
- Corbel, S., Tomsick, J.A., Kaaret, P. 2005, *ApJ*, in press, astro-ph/0509870
- De Young, D.S. 2002, *The Physics of Extragalactic Radio Sources* (Chicago, University of Chicago Press)
- Dickey, J.M. & Lockman, F.J. *ARA&A*, 28, 215
- Heinz, S. & Sunyaev, R. 2002, *A&A*, 390, 751
- Jones, C. 1977, *ApJ*, 214, 856
- Kaaret, P. 2005, *ApJ*, 629, 233
- Mason, K.O., Parmar, A.N., & White, N.E. 1985, *MNRAS*, 216, 1033
- Mathis, J.S., Mezger, P.G., & Panagia, N. 1983, *A&A*, 128, 212
- McClintock, J.E., Canizares, C.R., & Hiltner, W.A. 1978, *IAU Circ.* 3251
- Migliari, S. et al. 2002, *Science*, 297, 1673
- Mirabel, I.F. & Rodríguez, L.F. 1999, *ARA&A*, 37, 409
- Pan, H.C. et al. 1995, *MNRAS*, 274, L15
- Park, S.Q. et al. 2005, *ApJ*, 618, L45
- Roberts, M.S.E., Michelson, P.F., Cominsky, L.R., Marshall, F.E., Corbet, R.H.D., Smith, E.A. 1996, *IAU Circ.* 6302
- Safi-Harb, S. & Petre, R. 1999, *ApJ*, 512, 784
- Sault R.J. & Killeen N.E.B. 1998, *The Miriad User's Guide*, Sydney: Australia Telescope National Facility
- Strong, A.W., Moskalenko, I.V., Reimer, O. 2000, *ApJ*, 537, 763

- Wachter, S. & Smale, A.P. 1998, ApJ, 496, L21
- Watson, M.G., Willingdale, R., Grindlay, J.E., & Seward, F.D. 1983, ApJ, 273, 688
- Watson, M.G. et al. 1986, MNRAS, 222, 261
- White, N.E. et al. 1984, ApJ, 283, L9
- White, N.E. & Marshall, F.E. 1984, ApJ, 281, 354
- Wilms, J., Allen, A., McCray, R. 2000, ApJ, 542, 914